

Evidence for False Vacuum States inside the Cores of Massive Pulsars and the Ramification on the Measurements of Their True Masses

Ahmad A. Hujeirat*, Mauritz M. Wicker

IWR, University of Heidelberg, Heidelberg, Germany
Email: *AHujeirat@urz.uni-heidelberg.de

How to cite this paper: Hujeirat, A.A. and Wicker, M.M. (2023) Evidence for False Vacuum States inside the Cores of Massive Pulsars and the Ramification on the Measurements of Their True Masses. *Journal of Modern Physics*, 14, 1409-1425.
<https://doi.org/10.4236/jmp.2023.1411081>

Received: September 10, 2023

Accepted: October 16, 2023

Published: October 19, 2023

Copyright © 2023 by author(s) and Scientific Research Publishing Inc.
This work is licensed under the Creative Commons Attribution International License (CC BY 4.0).
<http://creativecommons.org/licenses/by/4.0/>



Open Access

Abstract

Based on the theory and observations of glitching pulsars, we show that the ultra-cold supranuclear dense matter inside the cores of massive pulsars should condensate in vacua, as predicated by non-perturbative QCD. The trapped matter here forms false vacuums embedded in flat spacetimes and completely disconnected from the outside world. Although the vacuum expectation value here vanishes, the masses and sizes of these incompressible superfluid cores are set to grow with cosmic times, in accord with the Onsager-Feynman superfluidity analysis. We apply our scenario to several well-studied pulsars, namely the Crab, Vela, PSR J0740+6620 and find that the trapped mass-contents in their cores read $\{0.15, 0.55, 0.64\}$, implying that their true masses are $\{1.55, 2.35, 2.72\} M_{\odot}$, respectively. Based thereon, we conclude that: 1) The true masses of massive pulsars and neutron stars are much higher than detected by direct observations and, therefore, are unbounded from above, 2) The remnant of the merger event in GW170817 should be a massive NS harbouring a core with $1.66 M_{\odot}$.

Keywords

Numerical Relativity, Pulsars, Magnetars, Neutrons Stars, Black Holes, Quantum Vacuum, QCD, Condensed Matter, Incompressibility, Superfluidity, Super-Conductivity

1. Introduction

Massive pulsars, magnetars and young neutron stars belong to the family of ultra-compact objects (UCOs), that liberate the content of energy left over from the collapse of their progenitors mainly through magnetic dipole radiation at the

rate: $\dot{E}_{MDR} \sim B^2 \Omega^4$, where B, Ω are the magnetic field intensity and angular frequency, respectively [1] [2] [3].

For typical values of Ω and B , the energy losses amount to roughly one million times larger than the luminosity of the Sun, and therefore their luminous lifetime (-LLT) is expected to be one million times shorter [1]. Similar to normal stars, massive NSs are much more compact and cool faster than their low-mass counterparts [4]. This may explain why the NSs formed from the first generation of massive stars are missing; It is because they just became invisible or they collapsed into black holes (see [5], and the references therein). However, the NS-merger event in GW170817 clearly argues against the collapse scenario, as to date there is no exclusive evidence that the remnant ended its life in BH [6] [7] [8] [9]. The ultimate fate of the remnant depends solely on the physical properties of matter making up the cores of massive NSs. Numerical modellings of the internal structure of massive NSs unambiguously show that matter must be cold and its density is far beyond the saturation value ρ_0 , which is the regime of non-perturbative quantum chromodynamics, QCD [10] [11].

However, the physical conditions governing the matter inside the cores of NSs are by no means reproducible in labs, so its true nature remains a matter of speculation. On the other hand, based on theoretical and observational constraints, it was argued that the energy density in the universe most likely is upper-bounded by the universal maximum $\langle \mathcal{E} \rangle_{max}^{uni} = \mathcal{O}(10^{35})$ erg/cc and lower-bounded by $\langle \mathcal{E} \rangle_{min}^{uni} = \mathcal{O}(10^{-9})$ erg/cc [12]. While the lower-bound corresponds to the cosmological vacuum, the upper-bound here corresponds to the fluid state, in which incompressible and entropy-free supranuclear dense matter undergoes a collective condensation in QCD-vacuum.

In the present study, we show that this matter with $\mathcal{E} = \langle \mathcal{E} \rangle_{max}^{uni}$ should be in a superfluid state trapped in a false vacuum field and embedded in flat spacetime. While the matter-field system is metastable on super-cosmic times, it may still decay into the true vacuum energy state via a hadronization process and the formation of a giant fireball.

2. The Fate of Ultra-Cold Supranuclear Dense Matter in NSs

As the secondary energies¹ in UCOS² are relatively small compared to the rest energy, one may safely assume the embedding spacetime to be Schwarzschild. When integrating the TOV equation from outside-to-inside using appropriate EOSs, one immediately encounters the regime, where density surpasses the nuclear saturation density ρ_0 . However, the microphysics governing the state of matter in the density regime $[\rho \geq 1.5\rho_0]$ is poorly understood and completely uncertain [3]. Unlike terrestrial conditions, where the accelerated particles consist roughly of an equal number of neutrons and protons, the electron-capturing by protons in the above-mentioned regime is highly asymmetric. Therefore in

¹*I.e.* all energies other than the rest energy.

²To the Ultra-Compact Objects belongs the whole family of neutron stars, e.g. pulsars and magnetars.

the absence of a reliable, effective mesonic theory from QCD, one relies on smooth extrapolation from the lower density regime to predict the state of matter in the supranuclear density regime. Such approaches are risky and unsuited to explore anomalies or abrupt transitions into new or exotic states [13] [14].

Based thereon, it is not unreasonable to argue that there might be a critical density, $\rho_{cr} \approx 3\rho_0$, at which the matter reaches maximum compressibility and then goes promptly into a purely incompressible phase. Among others, the following arguments support this hypothesis:

- NSs are spherically symmetric and static objects. Hence the physical variables must fulfil the regularity condition at the center, *i.e.* $\nabla\mathcal{E}|_{r=0} = 0$, where \mathcal{E} is the energy density. This condition is equivalent to requiring the fluid to be incompressible at $r=0$. For quantum fluids, positions are uncertain and they should be replaced by intervals $r \rightarrow \langle r \rangle = \Delta r = c/\Delta t$. Hence, using the uncertainty principle, the regularity condition is equivalent to:

$$0 \approx \frac{\Delta\mathcal{E}}{\Delta r} \geq \frac{\hbar}{2} \frac{c}{\Delta r^2}. \quad (1)$$

This implies that Δr must be of macroscopic length scale and specifically larger than 2.41×10^3 cm. For $\rho \approx \rho_{cr}$, we obtain a mass of $2.4 \times 10^{-8} M_\odot$, which should be the initial mass of the embryonic incompressible core of newly born pulsars. As clarified later, the core's matter should be in an incompressible superfluid state.

- At $\rho \geq 1.5\rho_0$ nucleons come into touching, where nuclear forces dominate, and the gravitational force becomes negligibly small. Following [15], at zero-temperature and critical density $\rho_{cr} = 2.938\rho_0$, the nucleons merge together to form a sea of incompressible gluon-quark superfluid. This argument, as it will be clarified later, is in line with the recent NICER and XMM-Newton observations of the massive magnetar PSR J0740+6620, whose mass and radius are predicted to be $2.08 \pm 0.07 M_\odot$ and $R_* = 13.7 \pm 1.5$ km, respectively. In **Figure 1**, we show the internal structure of the pulsar by solving the TOV equation using a variety of EOSs. Obviously, almost all EOSs (see **Figure 2** and **Appendix** for further details) appear to converge to ρ_{cr} , but then start diverging strongly as $\rho = 5\rho_0$ is approached. A reasonable explanation would be that once the gravitational field has compressed the hadrons up to the critical supranuclear density, ρ_{cr} , the confining membranes of individual hadrons start overlapping, and the frozen quarks at zero-temperature start behaving as electrons in metal; the attractive force between them may trigger a collective Cooper-pairing, which turns the quark into an incompressible superfluid [3] [16]. Indeed, although the physical conditions governing particle collisions in labs are radically different from those in the cores of massive NSs, the resulting medium from the heavy ion collisions at the RHIC was found to behave as a nearly perfect fluid, where the viscosity relative to entropy, η/s , was close to the conjectured lower-bound [17] [18] [19] [20]. We note here that further compression of the superfluid

by gravity is unnecessary, as it would considerably enhance the object’s compactness, which then counters observations [21].

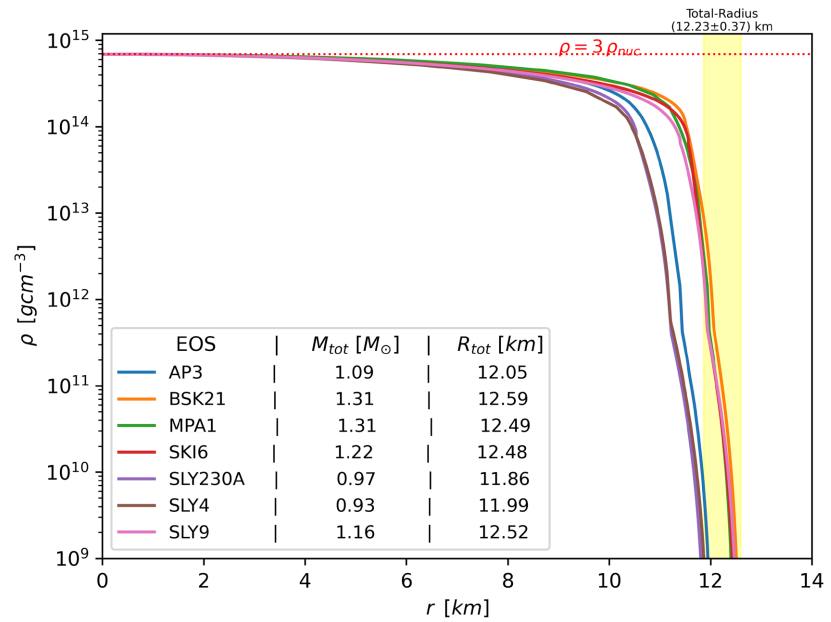


Figure 1. The predicated lower-limit of pulsar’s masses that don’t succeed to form significant SuSu-cores, where the material density attains its universal maximum $\rho_{cr} = 3\rho_0$. Newly born pulsars with a compactness parameter larger than $\alpha_{co} = 0.28$ would give rise to the formation of embryonic cores, whose mass and dimension would grow as they evolve on cosmic times.

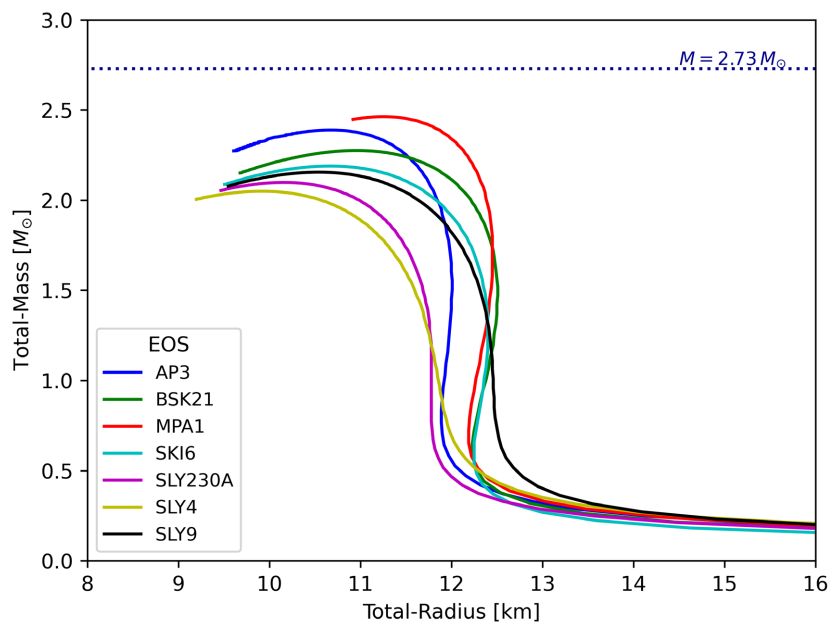


Figure 2. The credibility of modelling the internal structure of NSs using known EOSs is limited by a maximum mass of roughly $2.5M_{\odot}$. Assuming the remnant of the merger event in GW170817 is a massive NS, then its internal structure is far beyond the regime of validity of these EOSs.

- Young pulsars have been observed to spin at much higher rates than their old counterparts [22] [23]. Indeed, the initial rotational frequency of newly born pulsars was predicated to be around 1540/s [24]. The bulk of rotational energy in these newly born pulsars is carried mainly by the compressible and dissipative matter surrounding the central embryonic cores. Following [25], isolated pulsars are expected to glitch approximately 10 billion times during their luminous lifetime, and the repetition of the glitch events decreases with increasing the mass and age³. Our glitch scenario of pulsars predicts that superfluid cores should deposit certain amounts of their rotational energies into the ambient media abruptly, where they are then absorbed and subsequently redistributed viscously and to show up as sudden spin-ups of pulsars. Based thereon, the cores can be neither static nor be the only source of rotational energy, E_{rot} , as otherwise they would run out of E_{rot} after a certain number of glitches. In this case, we may apply the Onsager-Feynman equation of superfluidity to study the dynamics of the core during the glitch events:

$$\oint \mathbf{v} \cdot d\mathbf{l} = \frac{2\pi}{m} N, \tag{2}$$

where v, N, ℓ are the angular velocity, number of enclosed vortices and line-element of the path enclosing the vortices. As glitching are discrete events in time, we may transform the equation into the finite discretization space so that spatial changes can be measured in slices of time as follows:

$$\left(\frac{d(S\Omega)}{dt} = \frac{\hbar}{2m} \frac{dN}{dt} \right) \xrightarrow{\text{Finite space-time}} \frac{(S\Omega)^{n+1} - (S\Omega)^n}{\Delta t} = \frac{\hbar}{2m} \left(\frac{N^{n+1} - N^n}{\Delta t} \right), \tag{3}$$

where $\Delta t (\doteq t^{n+1} - t^n)$ is the time interval between two successive glitch events, and $\{S, \Omega, N\}_{n=1}^\infty$ are sequences of discrete elements consisting of the cross-sections, rotational frequencies and the enclosed number of vortices, respectively. The RHS of Equation (3) measures the number of deposited vortex lines that subsequently redistributed viscously in the shell. It is reasonable to assume that the RHS of Equation (3) remains relatively small, which requires $N^{n+1} \approx N^n$. The underlying reasonings may read: As the rotational energy, E_{rot} , of a newly born pulsar is distributed almost uniformly throughout the entire object, then the superfluid core should entail a negligibly small fraction of E_{rot} . Thus, the core cannot indefinitely supply the ambient medium with E_{rot} via glitching for a substantial period of the pulsar’s lifetimes. As cores grow with cosmic times, the matter that joins the core during glitching must adjust its physical properties to those in the core. Here the boundary layer is best suited, where the adaptation mechanism could operate, including cultivating δN^+ low energetic vortex lines that should join the core during a glitch event. This number should be comparable to the number of expelled vortex lines, δN^- , so that the nett difference remains small (see **Figure 3**). To be noted here that $\left| \frac{d\Omega}{dr} \right|$ peaks inside the boundary

³The Vela pulsar is roughly ten times older than the Crab, and the duration between two successive glitch events of Vela is roughly 1.66 longer than of the Crab.

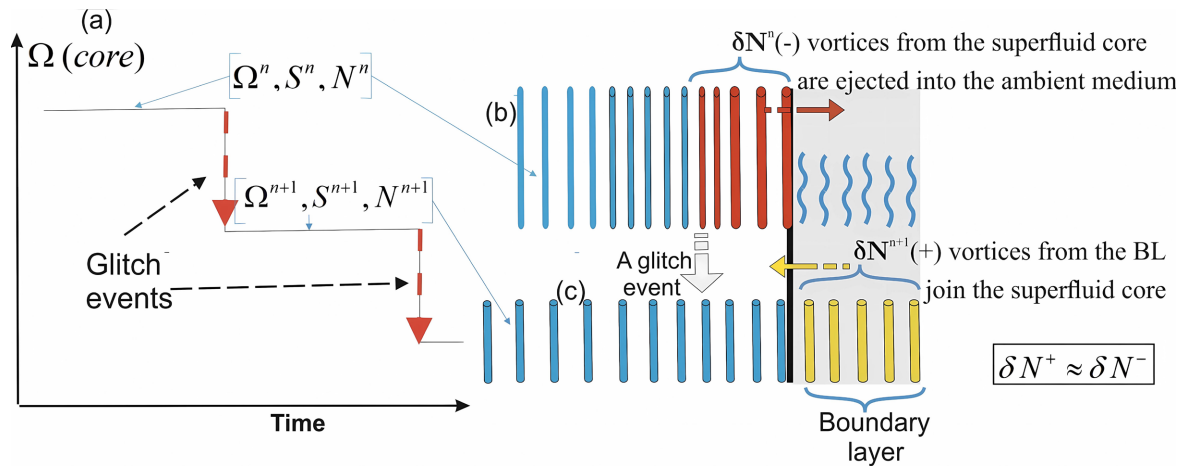


Figure 3. In (a), two arbitrary discrete levels of the angular frequency, Ω^n and Ω^{n+1} , the corresponding cross-sections S^n and S^{n+1} and the enclosed number of vortex lines N^n and N^{n+1} are shown. The glitch event is defined when the core undergoes an abrupt transition from a high, Ω^n to a low angular frequency level Ω^{n+1} , which is associated with an ejection of a certain number of vortices into the ambient medium (red tubes in b). The ejected powerful vortices are replaced by low energetic ones (yellow tubes in c), that are created in the boundary layer between the core and the surrounding shell.

layer (BL), where the dynamo action could operate efficiently. This picture is remarkably similar to the solar tachocline, where the solar dynamo is considered to operate efficiently.

Consequently, Equation (3) implies that:

$$\frac{dS}{dt} \approx -\frac{d\Omega}{dt} > 0 \tag{4}$$

Hence the cross-section of the core increases with each glitch event, and therefore the core doesn't obey the mass-radius relation that generally applies to UCOs. Note that imposing the zero-torque condition on the core, *i.e.*, $\frac{d}{dt}(\Omega I_{core}) = 0$ strengthens our conclusion.

3. ³SuSu-Matter and the Spacetime Topology

In the following, we show that the topology of spacetime embedding incompressible, entropy-free supranuclear dense superfluid, *i.e.* SuSu-matter, must be flat.

■ **Theorem:**

The spacetime embedding incompressible SuSu-matter must be flat

Proof: Assume we are given a static and spherically symmetric core made of incompressible SuSu-fluid. Following Birkhoff's theorem, the spacetime surrounding the core should be Schwarzschild. Furthermore, let us assume that this Schwarzschild spacetime accepts analytical continuation, so that it can be extended inwards into the core. Adopting the classical definition of pressure:

$P = -\frac{d\mathcal{E}}{dVol}$, where $dVol$ is a volume element, and integrating the TOV-equation:

$$\frac{dp}{dr} = -(\mathcal{E} + p) \frac{dV}{dr} = -\frac{\mathcal{E} + p}{r^2} \frac{m(r) + 4\pi r^3 p}{1 - \alpha_c(r)}, \tag{5}$$

then the following analytical solution may be obtained [2]:

$$\beta_p = \frac{P}{\mathcal{E}_0} = \frac{\sqrt{1-\alpha_c^0} - \sqrt{1-\alpha_c^0 r^2}}{\sqrt{1-\alpha_c^0 r^2} - 3\sqrt{1-\alpha_c^0}}, \tag{6}$$

where $\mathcal{V}, \alpha_c (\doteq m(r)/r), \mathcal{E}_0$ are the exponent of the metric coefficient g_{00} , the dynamical compactness parameter and the reference constant energy density, respectively. Here $\alpha_c^0 = \alpha_c^0(r=R_*)$. In **Figure 4**, we show that β_p increases as the centre is approached, and in most cases, it becomes ultrabaric, where the causality condition is grossly violated. Moreover, the pressure becomes a global rather than a local thermodynamical quantity, as dictated by the first law of thermodynamics.

In terms of the chemical potential, $\mu(r) (\doteq d\mathcal{E}/dp)$, the integration of the TOV equation in general yields $\mu(r)e^\mathcal{V} = const$. In the present incompressible case, this applies that $\mu(r) = const$ and therefore $\mathcal{V} = const$. Recalling that $e^\mathcal{V} \rightarrow 1$ as $r \rightarrow \infty$, we conclude that $\mathcal{V} = 0$.

This implies that curved spacetimes force fluids to stratify, even when the concerned fluid is incompressible. Noting that the weight of the column density starting at the core’s boundary increases toward the centre, *i.e.*:

$$\Sigma_{core} = \int_{r_{core}}^{R_*} \rho dz < \Sigma_* = \int_{r=0}^{R_*} \rho dz. \tag{7}$$

This inward enhancement of compression would break the rigidity of the condensate and convert the coherent motion into a differential one, practically destroying its superfluidity. Based thereon, we conclude that dynamically stable incompressible SuSu-matter requires the pressure also to be uniform everywhere.

The relevant question here is: Does the flat spacetime inside the incompressible cores of NSs match smoothly with the surrounding curved spacetime?

Here we propose the following *corollary*:

■ **The Flat spacetimes embedding SuSu-cores of massive NSs are self-contained and topologically disconnected from ambient spacetimes.**

Proof: Using Birkhoff’s theorem, the deviation between the metric coefficients of Minkowski-flat and Schwarzschild-curved spacetimes as well as of their derivatives read:

$$\begin{aligned} \Delta_{00} = \eta_{00} - g_{00} = \alpha_c r^2, \quad \Delta_{11} = \eta_{11} - g_{11} &= \frac{1}{\frac{1}{\alpha_c r^2} - 1} \\ \Delta'_{00} = \eta'_{00} - g'_{00} = 2\alpha_c r, \quad \Delta'_{11} = \eta'_{11} - g'_{11} &= \Delta'_{00} \frac{1-\varepsilon}{(1-\alpha_c r^2)^2}, \end{aligned} \tag{8}$$

where $\varepsilon \ll 1$ is a small number. Clearly, $\Delta_{00}, \Delta'_{00}, \Delta_{11}, \Delta'_{11}$ converge to zero if and only if $r \rightarrow 0$, *i.e.* there is no physical core with a reasonable radius across which both metrics could match smoothly.

In **Figure 5**, the mismatch of both spacetimes is illustrated schematically. It should be noted, however, that this macroscopic feature appears to apply all the

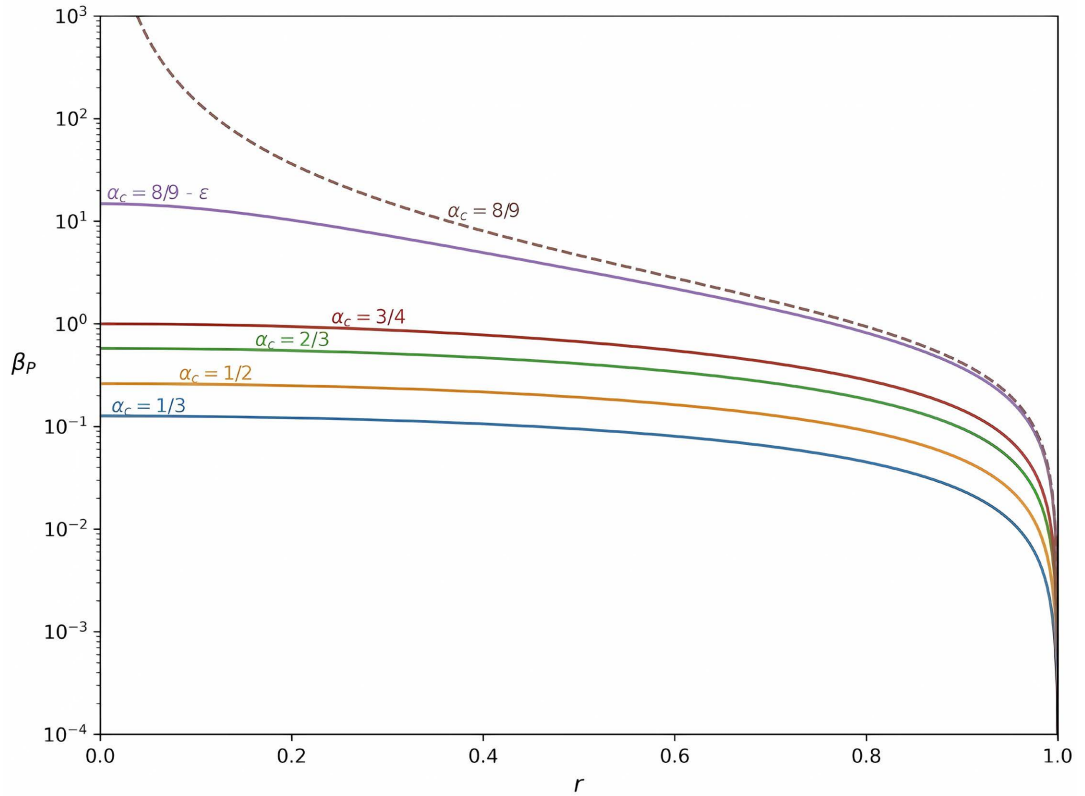


Figure 4. The radial distribution of the relative pressure of the incompressible fluid versus radii for different values of the compactness parameter $\alpha_c (\doteq R_s/R)$ at the background of Schwarzschild spacetimes. Although purely incompressible fluid doesn't accept stratification, the considerable increase of the pressure inwards forces the fluid to stratify and turns it into ultrabaric matter, which does not respect causality.

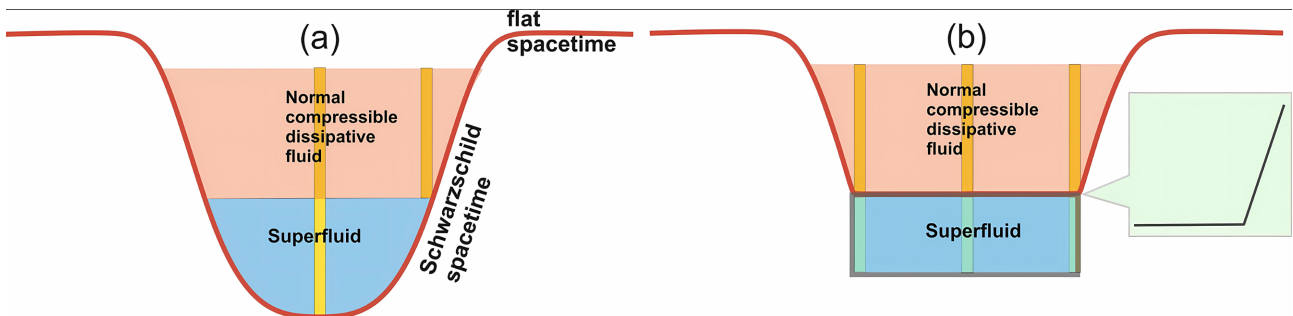


Figure 5. A schematic description of a normal compressible and dissipative fluid in a shell (orange coloured region) surrounding a core of a superfluid embedded in a Schwarzschild spacetime (blue coloured region in a). In (b), the superfluid is set to be embedded in flat spacetimes, though the transition between the two spacetimes is continuous but not differentiable.

way down to the quantum scales, as the gluon-quark clouds and their embedding spacetime topologies inside individual hadrons are invisible to observers situated in the surrounding curved spacetimes.

The Trapped SuSu-Matter inside False Vacuums

In the previous section, we have shown that the cores of pulsars and NSs most likely are made of incompressible SuSu-superfluids embedded in Minkowski flat

spacetimes. The spacetimes inside and outside SuSu-cores are topologically disconnected, and therefore two reference frames are needed to collect information to study massive NSs. Inside the cores, all observers would perceive the entire surrounding as perfectly homogeneous and isotropic, independent of their positions. We even conjecture that these observers would not recognize the boundary of the core from inside, as the 2D surface would serve as a holograph [26] [27], where the information about the entire constituents are encoded and mirrored inward so that the observers see the core as if it were infinitely large homogeneous and isotropic universe.

In the weak field approximation, the gravitational potential inside the core is obtained by solving the Poisson equation for non-zero energy density:

$$\Delta\Phi = \frac{4\pi G}{c^2} \langle \mathcal{E} \rangle_0 = \text{const} \neq 0. \quad (9)$$

Clearly, no Lorentz-invariant Φ fulfils the equation. However, if Φ is an indirect measure for the deviation of the mean energy density from a universal background mean quantity, then we obtain:

$$\Delta\Phi = \frac{4\pi G}{c^2} (\langle \mathcal{E} \rangle - \langle \mathcal{E} \rangle_0). \quad (10)$$

When the physical condition pushes the normal matter into SuSu-state, where $\langle \mathcal{E} \rangle = \langle \mathcal{E} \rangle_0 = 3\rho_0 c^2 = \mathcal{O}(10^{35})$ erg/cc, then the gravitational potential Φ must vanish⁴, which means that the matter in this phase is in a gravitationally passive state. In GR, this corresponds to the equation:

$$R_{\mu\nu} - \frac{1}{2} R g_{\mu\nu} = \frac{8\pi G}{c^4} (T_{\mu\nu} - T_{\mu\nu}^0), \quad (11)$$

where $R, R_{\mu\nu}, T_{\mu\nu}$ are the Ricci scalar, Ricci tensor and the stress-energy tensor (SET), respectively. The equivalence of the last two equations in the weak field approximation requires that:

$$T_{\mu\nu}^0 = \langle \mathcal{E} \rangle_0 \times \eta_{\mu\nu}, \quad (12)$$

where $\eta_{\mu\nu}$ corresponds to the Minkowski-metric. This is similar to the cosmological vacuum, \mathcal{E}_{vac} , where the SET reads:

$$T_{\mu\nu}^{vac} = \mathcal{E}_{vac} \times \eta_{\mu\nu}. \quad (13)$$

Although $T_{\mu\nu}^0$ and $T_{\mu\nu}^{vac}$ apply for completely different regimes⁵, the transitions from one state to another are not smooth, but discontinuous and occur abruptly [12] [29] [30].

The state of matter in which $\langle \mathcal{E} \rangle = \langle \mathcal{E} \rangle_0$ may be classified as a false vacuum, as, on cosmological time scales, it is not immune against decay into the true vacuum state \mathcal{E}_{vac} . In the latter case, normal particles may gain mass through interactions with the superimposed Higgs field, which in turn, curves the embed-

⁴ $\Phi \rightarrow 0$ as $r \rightarrow \infty$.

⁵ $\frac{\langle \mathcal{E}_0 \rangle}{\mathcal{E}_{vac}} = \mathcal{O}(10^{45})$.

ding spacetime. The curvature then compresses the matter and facilitates its transition into the false vacuum state via condensation, which subsequently decay into normal matter via runaway hadronization processes. These cyclic events are schematically described in **Figure 6**.

As mentioned earlier, observers inside SuSu-cores cannot exchange information with the outside world. Here, not only the spacetimes are disconnected, but the embedding vacuum field as well. The energy states of the trapped matter corresponds to zero-point energy state $\Psi_0(x)$, which coincides with the vacuum state, $\Psi_v(x)$, and therefore the vacuum expectation value (vev) must vanish $\langle 0|\Psi|0\rangle=0$ and there is no spontaneous symmetry breaking on the particle scales. However, as in the core there is only one single length scale, *i.e.* its radius r_{core} , then the spatial dimensions of the macroscopic condensate, the embedding flat spacetime and the vacuum field are identical, we conclude that the trapped matter in vacuum, is not massless, but it should maintain its original mass prior to condensation. Under these conditions, the causality condition may allow the static condensate to ride a standing wave that oscillates in time, though not in space.

In fact, the energy density of this false vacuum falls nicely in the range of QCD vacuum:

$$10^{35} \frac{\text{erg}}{\text{cc}} \leq \mathcal{E}_{QCD}^{vac} \leq 10^{36} \frac{\text{erg}}{\text{cc}}. \tag{14}$$

Generally, at zero-temperature, the non-perturbative sector of QCD is highly non-linear and gives rise to gluon-quark condensates in vacuum, and therefore to non-zero vacuum expectation value $\langle 0|\bar{q}q|0\rangle \neq 0$ (see [11] [29] [30], and the references therein).

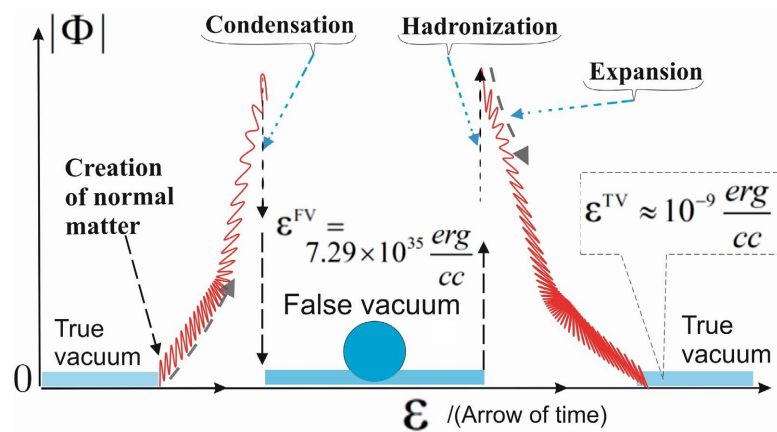


Figure 6. The cyclic evolution of the gravitational potential, Φ of vacuum-matter connection: the initial masses of elementary particles are created in certain vacuum fields with non-zero vev, but gain their measured masses through interactions with the Higgs field. The matter interacts with the embedding spacetime and evolves toward forming structures, including stars, UCOs etc. The matter in the cores of UCOs condensates in vacuum, forming thereby a false vacuum field, where Φ again vanishes. When the false vacuum decays via hadronization, Φ starts to gain significance but decreases as the system expands to finally reach the true vacuum, which governs the infinite parent universe [28].

Unlike our earlier discussion, the non-zero ν_{ν} here is a consequence of colour confinement and the presence of virtual quark-antiquark pairs and gluons in the vacuum state.

4. Revisiting the Masses of UCOs

In the previous sections, we argued that SuSu-matter making up the cores of massive NSs should be trapped in false vacuum fields. The spacetimes embedding these cores are flat, self-contained and disconnected from the outside world so that the actual mass of the cores are not communicated to outside observers. Consequently, the true mass of UCO, \mathcal{M}_{true} , reads:

$$\mathcal{M}_{true} = \mathcal{M}_{NM} + \mathcal{M}_{SuSu}, \quad (15)$$

where $\mathcal{M}_{NM}, \mathcal{M}_{SuSu}$ are the masses of normal matter (which determines the curvature of the embedding spacetime), and of the SuSu-matter (which communicates neither with the surrounding spacetimes nor with the surrounding quantum fields). This implies that the revealed masses of UCOs from observations correspond solely to normal matter, whereas the mass contents of their cores, \mathcal{M}_{SuSu} , remain undetected. Thus, the here-presented scenario introduces a new parameter, whose determination is challenging for both astronomers and theoreticians.

In the present study, the radius of the SuSu-core is set to be equal to the radius, at which the density of hadrons equals or surpasses the critical density $\rho_{cr} = 3\rho_0$, *i.e.*

$$r_{SuSu} \approx r(\text{at which } \rho = \rho_{cr}).$$

Based thereon, the following solution strategies are adopted:

- For a given pulsar and a fixed mass of normal matter, \mathcal{M}_{NM} , the TOV equation is solved numerically using a variety of EOSs.
- The true radius of the pulsar, or equivalently, the outer radius, is a nonlinear function of mass of normal matter, EOS and of ρ_{cr} , *i.e.*

$$R_* = f(\mathcal{M}_{NM}, \text{EOS}, \rho_{cr}), \quad (16)$$

which is solved iteratively.

- The mass of the SuSu-core is calculated through the integral:

$$\mathcal{M}_{SuSu} = 4\pi \int_0^{r_{SuSu}} \rho_{cr} r^2 dr. \quad (17)$$

To validate this approach, we apply our scenario to the three well-studied objects: The Crab, Vela and to the massive magnetar PSR J0740+6620 (**Figures 7-9**) and finally to the remnant of the NS-merger event in GW170817. In **Figure 9**, the density versus radius for the PSR J0740+6620 is plotted, where different EOSs are used. As usual, the TOV equation here is integrated from inside-to-outside, while iterating on the central density to obtain the total mass of the object revealed from observations. These results are to be compared with our scenario shown in **Figure 9**. Here we place a SuSu-core at the centre of the pulsar.

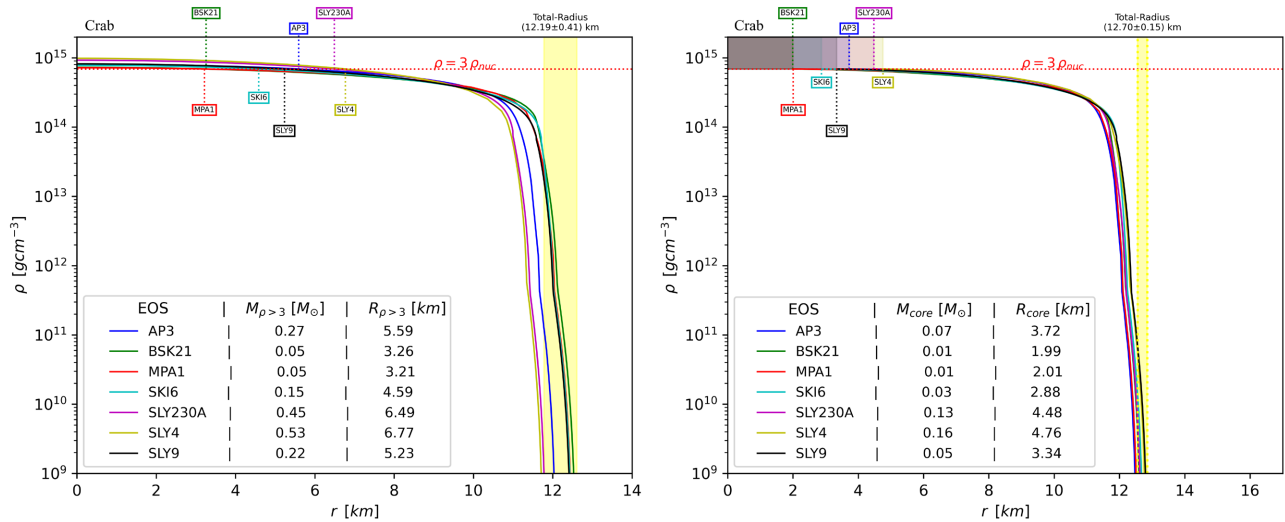


Figure 7. The radial distribution of the density inside the Crab-pulsar without (left panel) and with a SuSu-core (right panel), using various EOSs. The compactness parameter of the pulsar decreases with increasing the mass of the core. The profiles depart from each other in the absence of the SuSu-core, whereas the agreement is obvious when the SuSu-core is included.

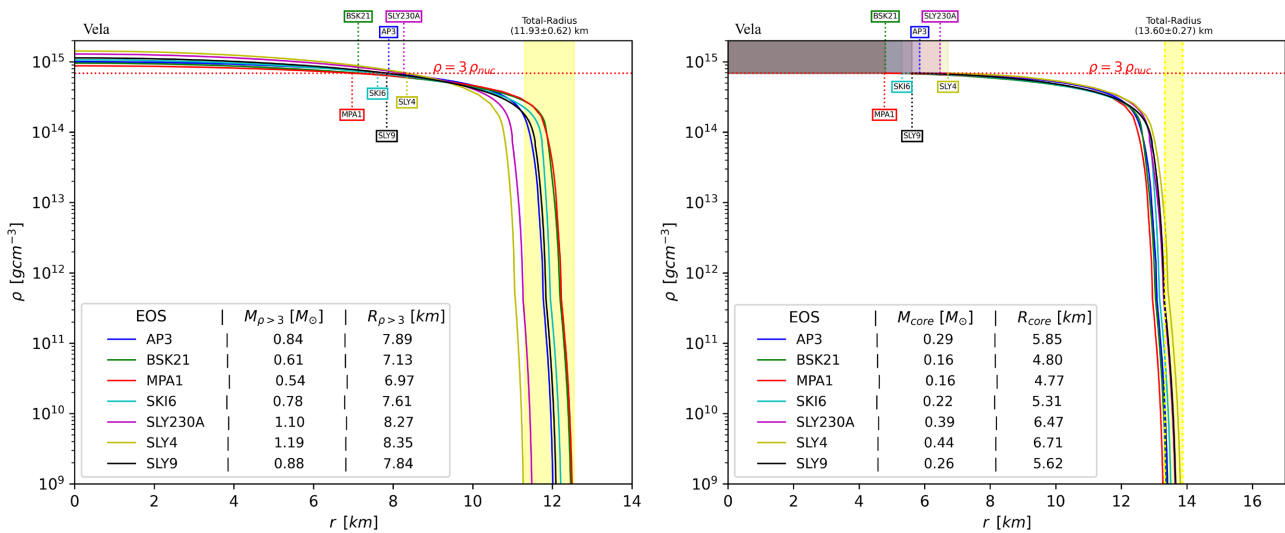


Figure 8. The radial distribution of the density inside the Vela-pulsar with (right panel) and without a SuSu-core (left panel), using various EOSs. The pulsar is clearly less compact with a central SuSu-core than otherwise. The agreement & disagreement between the profiles is similar to that in the Crab pulsar.

On the right panel, the compactness parameter, α_{co} , of several pulsars with and without SuSu-cores as a function of mass content of normal matter, is shown. While α_{co} increases almost linearly with the mass of normal matter, it saturates around 0.4, when incompressible SuSu-cores are included. The effect of flattening of the embedding spacetime by SuSu-cores is remarkably strong. In the right panel we tabulated the total predicted total mass of objects, namely the Crab, Vela, PSRJ0740+6620 as well as of the remnant of GW170817.

The distribution of the normal matter in the surrounding shell is obtained through integrating the TOV equation from outside-to-inside, using various

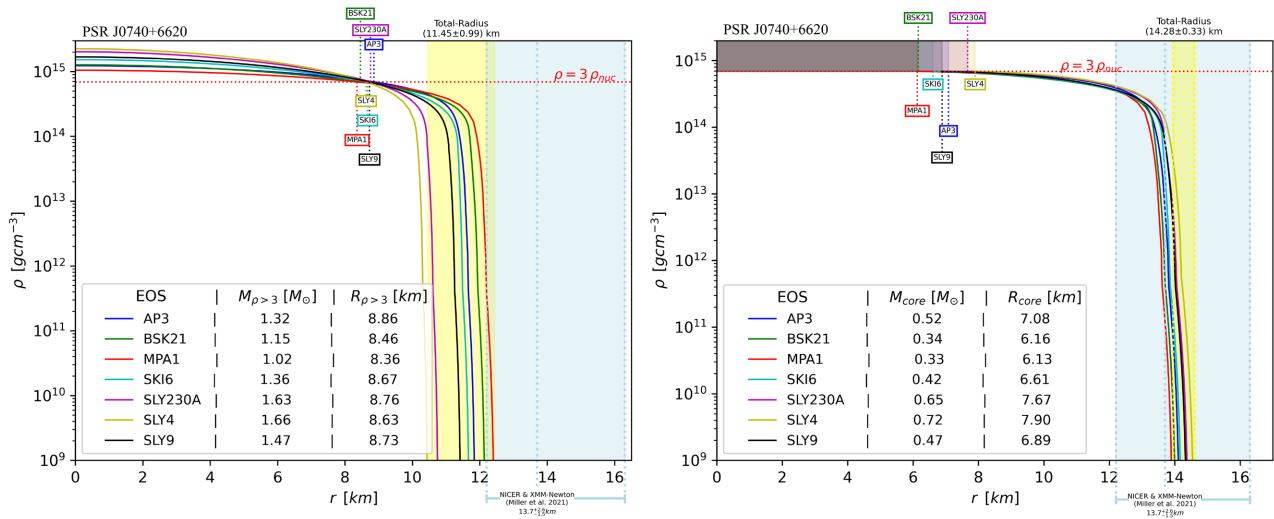


Figure 9. Similar to the previous figures: The radial distribution of the density inside the massive pulsar PSR J0740+6620 with (right panel) and without a SuSu-core (left panel), using various EOSs are shown. The difference between the compactness parameter of the pulsar with a central SuSu-core and without is remarkably strong. Also, the disagreements between the EOSs peak when more massive pulsars are considered, though there is an obvious agreement on the radius of this pulsar.

EOSs. The mass range of the SuSu-core was found to lie in the interval: $[0.33M_{\odot} \leq \mathcal{M}_{SuSu} \leq 0.72M_{\odot}]$, whereas the outer radius of the pulsars is 14.28 ± 0.33 km, which corresponds to a compactness parameter $\alpha_{cp} = 0.43 \pm 0.01$. Indeed, the radius of PSR J0740+6620 obtained using our scenario falls nicely in the range of radii revealed from NICER and XMM-Newton data, namely: $13.7^{+2.6}_{-1.5}$ km.

In the case of GW170817, we show in **Figure 10** that the remnant could be an extraordinarily massive and dynamically stable NS, supported by a central massive incompressible SuSu-core of $[0.97M_{\odot} \leq \mathcal{M}_{SuSu} \leq 1.62M_{\odot}]$. The radius of the remnant NS is predicated to be 15.90 ± 0.43 km.

It is worth mentioning here that, unlike normal viscous fluid flows, when two lumps of superfluids are set to pass each other, they may still retain their shapes and energies. Indeed, following [31], it was shown numerically that the superfluid cores of two NSs in GW170817 could merge to form a much more massive one with minimum energy loss (energy loss is due to numerical diffusion in the finite space). This a consequence of the low energy states of both cores, where there is no energy to lose.

As none of the EOSs is capable of modelling massive pulsars or young NSs with $\mathcal{M} \geq 2.1M_{\odot}$ that are made of purely normal matter, the formation of incompressible SuSu-cores appears to overcome this barrier, as the effects of SuSu-cores are also to flatten the curvatures of the embedding spacetimes and enable UCOs to be much more massive than could be detected by direct observations (see **Figure 10**).

We note here that the comparison of our results with the observations of glitching pulsars is based on data that have been obtained during recent years. Therefore they are selected snapshots that may not reflect the stationary structures of these UCOs.

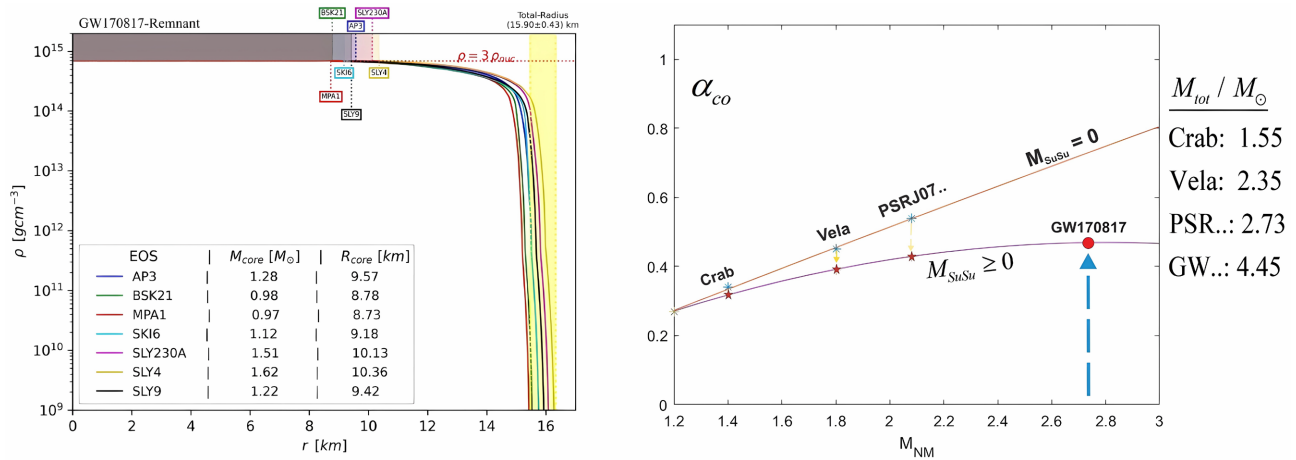


Figure 10. Left panel: The radial distribution of the density inside the remnant NS predicted to have formed during the NS-merger event in GW179817, for various EOSs. The remnant consists of a $2.73M_{\odot}$ massive shell made up of normal compressible and dissipative matter, which determines the topology of the embedding spacetime. Thereunder, the NS harbours a $1.6M_{\odot}$ massive SuSu-core, yielding a total remnant’s mass of $M \geq 4.0M_{\odot}$. Although this mass of the remnant is far beyond the classical mass range of NSs, the agreement between the EOSs, even in this exceptional case, is indeed remarkable.

To clarify the point here: our scenario requires that the amount of normal matter in the shell surrounding SuSu-cores should be sufficiently large so as to compress the matter at its base up to the critical value $\rho_{cr} = 3 \times \rho_0$. In the case of the Crab, Vela and PSR J0740+6620 the corresponding compactness parameters, α_{cp} are larger than 0.28. This implies that there is an ongoing conversion of normal matter into SuSu-matter, through which the core becomes larger and more massive. On the other hand, in the absence of mass enrichment by external processes, such as accretion, merger, etc., objects with $\alpha_{co} \leq 0.28$ should enter inactive epochs in their evolution, thereby becoming invisible dark objects (DEOs). This may explain the missing large number of NSs in our Galaxy and those formed from the collapse of the first generation of stars.

We note also that although the magnetar PSR J0740+6620 is much more massive and closer than the Crab pulsar, it is not classified as a glitching pulsar. However, based on our scenario, the compactness parameter of this magnetar is much higher than 0.28 and therefore it should be glitching, though at a much higher frequency than observed in normal pulsars and most likely beyond the sensitivity of the currently used instrumentations.

5. Summary & Discussion

In this paper, we have shown that the cores of massive pulsars are most likely made of SuSu-matter trapped in false vacuums and embedded in flat spacetimes that underwent complete decoupling from the external world. We argued that a glitch event occurs in a geometrically thin boundary layer, where the core moves discretely from one angular frequency level to the next lower one and where the matter density surpasses the maximum compressibility limit of $\rho_{cr} = 3\rho_0$. In this regime, non-perturbative QCD applies and gives rise to a collective conden-

sation of matter, forming a false vacuum field.

For observers inside the core, the trapped matter in the field is purely incompressible, static, homogeneous, isotropic and metastable, thanks to the abrupt decoupling of the embedding spacetime and the vacuum field from the ambient world. However, this implies that the mass of the condensate cannot be communicated to outside observers, which means that the revealed masses of UCOs by direct observations of normal matter should be modified to include the mass of the cores.

We employed the here-presented scenario to several well-studied pulsars, namely the Crab, Vela and PSR J0740+6620 and found that, when the masses of the cores are included, then their masses should be 1.55, 2.35, 2.72 instead of 1.4, 1.8, 2.07 solar masses, respectively.

In the present study, we have also shown that: 1) the total masses of glitching pulsars with false vacuum cores are unbounded from above; therefore, NSs, whose masses surpass the $2.2M_{\odot}$ should not necessarily collapse into black holes. 2) The remnant of the NS-merger in GW170817 is predicted to be a massive NS harbouring a massive condensate in the core of roughly $1.66M_{\odot}$. 3) Massive black holes could in principle, be ultra-massive NSs with super-massive SuSu-cores trapped in false vacuum fields. 4) The progenitor of the Big Bang could have been a non-singular giant object made of SuSu-matter trapped in a false vacuum field [32]. On super-cosmic time scales, this giant object is not immune against decay and would turn into normal matter via a runaway hadronization process that ends up in a giant Big Bang explosion.

Acknowledgements

The IWR-KAUST cooperation project has financed this work.

Conflicts of Interest

The authors declare no conflicts of interest regarding the publication of this paper.

References

- [1] Shapiro, S.L. and Teukolsky, S.A. (1983) *Black Holes, White Dwarfs and Neutron Stars*. John Wiley & Sons, New York. <https://doi.org/10.1002/9783527617661>
- [2] Glendenning, N.K. (2007) *Special and General Relativity*. Springer, Berlin. <https://doi.org/10.1007/978-0-387-47109-9>
- [3] Camenzind, M. (2007) *Compact Objects in Astrophysics*. Springer, Berlin.
- [4] Hampel, M., Fischer, T., *et al.* (2012) *The Astrophysical Journal*, **748**, 70. <https://doi.org/10.1088/0004-637X/748/1/70>
- [5] Hujeirat, A.A. (2021) *Journal of Modern Physics*, **12**, 937-958. <https://doi.org/10.4236/jmp.2021.127057>
- [6] Abbott, *et al.* (2019) *Physical Review X*, **9**, Article ID: 011001.
- [7] Piro, L., Troja, E. and Zhang, B. (2019) *MNRAS*, **483**, 1912-1921.

- <https://doi.org/10.1093/mnras/sty3047>
- [8] Hujeirat, A. and Samtaney, R. (2020) *Journal of Modern Physics*, **11**, 1785-1798. <https://doi.org/10.4236/jmp.2020.1111111>
- [9] Ligo Cooperation (2023) Another Long Hard Look for a Remnant of GW170817. <https://www.ligo.org/science/Publication-GW170817PostMergerLong/index.php>
- [10] Veltman, M. (1975) *Physical Review Letters*, **34**, 777. <https://doi.org/10.1103/PhysRevLett.34.777>
- [11] Rugh, S.E. and Zinkernagel, H. (2000) *Studies in History and Philosophy of Modern Physics*, **33**, 663-705.
- [12] Hujeirat, A.A. (2023) *Journal of Modern Physics*, **14**, 790-801. <https://doi.org/10.4236/jmp.2023.146045>
- [13] Adam, C., Naya, C., *et al.* (2015) *Physical Review C*, **92**, Article ID: 025802. <https://doi.org/10.1103/PhysRevC.92.025802>
- [14] Baym, G., Hatsuda, T., *et al.* (2018) *Reports on Progress in Physics*, **81**, Article ID: 056902. <https://doi.org/10.1088/1361-6633/aaae14>
- [15] Hujeirat, A.A. (2018) *Journal of Modern Physics*, **9**, 51-69. <https://doi.org/10.4236/jmp.2018.91004>
- [16] Pethick, C.J., Schfer, T. and Schwenk, A. (2017) Bose-Einstein Condensates in Neutron Stars. In: Proukakis, N., Snoko, D. and Littlewood, P., Eds., *Universal Themes of Bose-Einstein Condensation*, Cambridge University Press, Cambridge, 573-592. <https://doi.org/10.1017/9781316084366.031>
- [17] Son, D.T. and Starinets, A.O. (2007) *Annual Review of Nuclear and Particle Science*, **57**, 95-118. <https://doi.org/10.1146/annurev.nucl.57.090506.123120>
- [18] Mueller, B. (2007) From Quark-Gluon Plasma to the Perfect Liquid.
- [19] LHCb Collaboration (2015) *Physical Review Letters*, **115**, Article ID: 072001.
- [20] Eskola, K.J. (2019) *Nature Physics*, **15**, 1111-1112. <https://doi.org/10.1038/s41567-019-0643-0>
- [21] Miller, M.C., Lamb, F.K., *et al.* (2021) *The Astrophysical Journal Letters*, **918**, L31.
- [22] Espinoza, C.M., Lyne, A.G., Stappers, B.W. and Kramer, C. (2011) *MNRAS*, **414**, 1679-1704. <https://doi.org/10.1111/j.1365-2966.2011.18503.x>
- [23] Roy, J., Yashwant Gupta, Y. and Lewandowski, W. (2012) *MNRAS*, **424**, 2213-2221. <https://doi.org/10.1111/j.1365-2966.2012.21380.x>
- [24] Haensel, P., Lasota, J.P. and Zdunik, J.L. (1999) *A&A*, **344**, 151.
- [25] Hujeirat, A. (2018) *Journal of Modern Physics*, **9**, 554-572. <https://doi.org/10.4236/jmp.2018.94038>
- [26] 't Hooft, G. (2000) The Holographic Principle.
- [27] 't Hooft, G. (2001) Basics and Highlights in Fundamental Physics. *Proceedings of the International School of Subnuclear Physics*, Erice, August-September 2000, 72-100. <https://doi.org/10.4236/jmp.2023.144023>
- [28] Hujeirat, A.A. (2023) *Journal of Modern Physics*, **14**, 415-431.
- [29] Zel'dovich, Y.B. (1968) *Soviet Physics Uspekhi*, **11**, 381-393. <https://doi.org/10.1070/PU1968v011n03ABEH003927>
- [30] Weinberg, S. (1989) *Review of Modern Physics*, **61**, 1-23. <https://doi.org/10.1103/RevModPhys.61.1>
- [31] Sivakumer, A., Muruganandam, P. and Hujeirat, A.A. (2023) On the Merger of Superfluid Cores of Neutron Stars and the Nature of the Remnant of GW170817. (In

Preparation)

- [32] Hujeirat, A.A. (2022) *Journal of Modern Physics*, **13**, 1474-1498. <https://doi.org/10.4236/jmp.2022.1311091>
- [33] Akmal, A., Pandharipande, V.R. and Ravenhall, D.G. (1998) *Physical Review C*, **58**, 1804-1828. <https://doi.org/10.1103/PhysRevC.58.1804>
- [34] Potekhin, A.Y., Fantina, A.F., Chamel, N., Pearson, J.M. and Goriely (2013) *A&A*, **560**, A48. <https://doi.org/10.1051/0004-6361/201321697>
- [35] Muether, H., Prakash, M. and Ainsworth, T.L. (1987) *Physics Letters B*, **199**, 469-474. [https://doi.org/10.1016/0370-2693\(87\)91611-X](https://doi.org/10.1016/0370-2693(87)91611-X)
- [36] Gulminelli, F. and Raduta, A.R. (2015) *Physics Letters C*, **92**, Article ID: 055803. <https://doi.org/10.1103/PhysRevC.92.055803>
- [37] Danielewicz, P., Lee, J. and Ad, R. (2009) *Nuclear Physics A*, **818**, 36-96. <https://doi.org/10.1016/j.nuclphysa.2008.11.007>
- [38] Reinhard, P.-G. and Flocard, H. (1995) *Nuclear Physics A*, **584**, 467-488. [https://doi.org/10.1016/0375-9474\(94\)00770-N](https://doi.org/10.1016/0375-9474(94)00770-N)
- [39] Chabanat, E., Bonche, P., *et al.* (1997) *Nuclear Physics A*, **627**, 710-746. [https://doi.org/10.1016/S0375-9474\(97\)00596-4](https://doi.org/10.1016/S0375-9474(97)00596-4)
- [40] Douchin, F. and Haensel, P. (2001) *A&A*, **380**, 151-167. <https://doi.org/10.1051/0004-6361:20011402>

Appendix

In the following, we list the EOSs used in the here-presented calculations.

- **AP3**: Variational-Method EOS with plain $npe\mu$ nuclear matter [33]
- **BSK21**: Non-relativistic Skyrme interaction based EOS with plain $npe\mu$ nuclear matter [34]
- **MPA1**: Relativistic Brueckner-HartreeFock EOSs with plain $npe\mu$ nuclear matter [35]
- **SKI6**: Non-relativistic Skyrme interaction based EOS with plain $npe\mu$ nuclear matter [36] [37] [38]
- **SLY230A**: Non-relativistic Skyrme interaction based EOS with plain $npe\mu$ nuclear matter [39]
- **SLY4**: Potential based EOS with plain $npe\mu$ nuclear matter [40]
- **SLY9**: Non-relativistic Skyrme interaction based EOS with plain $npe\mu$ nuclear matter [36] [37]